This article has been accepted for publication in IEEE Access. This is the author's version which has not been fully edited and content may change prior to final publication. Citation information: DOI 10.1109/ACCESS.2024.3494042

IEEE Access
Multidisciplinary | Rapid Review | Open Access Journal

Digital Object Identifier

Enhanced Process Monitoring for the Maxwell Process via the CUSUM Control Chart and its Application to the Carbon Fiber Industry

ZAHID KHAN[1], FAISAL SHAH[2], ATTILA I KATONA[3], and ZSOLT T. KOSZTYÁN,[4]
[1]Department of Quantitative Methods, University of Pannonia, H-8200 Egyetem str. 10, Veszprém, Hungary (e-mail:zahidkhan@hu.edu.pk)
[2]Department of Mathematics and Statistics, Riphah International University, Islamabad, Pakistan (e-mail: syedfaisalshah73@gmail.com)
[3]Department of Quantitative Methods, University of Pannonia, H-8200 Egyetem str. 10, Veszprém, Hungary (e-mail: katona.attila@gtk.uni-pannon.hu)
[4]Department of Quantitative Methods, University of Pannonia, H-8200 Egyetem str. 10, Veszprém, Hungary (e-mail: kosztyan.zsolt@gtk.uni-pannon.hu)

This work has been implemented by the TKP2021-NVA-10 project with support provided by the Ministry of Culture and Innovation of Hungary from the National Research, Development and Innovation Fund, financed under the 2021 Thematic Excellence Programme funding scheme.

ABSTRACT Control charts are the diagnostic tools used in statistical applications for detecting possible changes in a process. One of the effective approaches for identifying smaller shifts in the process under the memory control charts is the cumulative sum (CUSUM) chart. The ordinary CUSUM schemes are designed exclusively on the basis of the normality assumption, which may not hold true for many process quality characteristics in practical scenarios. To address this, the V_{SQ}-chart is frequently utilized for analyzing nonnormal data, with the purpose of detecting sudden changes in the scale parameter of the Maxwell process. However, the V_{SQ}-chart lacks sensitivity to smaller parameter changes. In this work, a novel extension of the V_{SQ}-chart called the Maxwell CUSUM (MXCUSUM) chart is designed to monitor small changes in a process that follows the Maxwell distribution. The MXCUSUM chart exhibits strong detection capabilities across a variety of smaller shift sizes. Through Monte Carlo simulations, the run length properties of the proposed chart are assessed and compared with those of other existing charts. The comparative analysis reveals that the MXCUSUM is more effective at detecting a range of small shift sizes than its existing counterpart is. Finally, two real-life examples are utilized to illustrate the design and implementation procedure of the proposed chart.

INDEX TERMS Skewing process, Maxwell distribution, Control chart, CUSUM chart, Run length, Estimation, Simulation.

I. INTRODUCTION

Control charts are a popular graphical tool for tracking statistical processes over time in many different uses. The charts serve as graphical tools used for identifying special events that may result in noticeable shifts in the process target [1]. Initially, developed for use in manufacturing, control charts now have practical applications in various fields, including environmental science, engineering, medicine, epidemiology, finance, athletics, genetics and law enforcement [2]. The goal of statistical process control (SPC) is to identify deviations from optimal performance and detect unpredictable variations before they cause defects and improve the production process [3]. This approach is used to maintain the stability of observed processes over time [4]. There are three primary types of control charts: Shewhart charts, cumulative sum (CUSUM) charts, and exponentially weighted moving average (EWMA) charts. The latter two are more advanced and can respond to small-to-moderate abrupt changes in process parameters faster than can Shewhart charts [5]. This makes them the preferred tool for monitoring statistical processes [6]. Several reviews of control charting methods have been conducted, including those by Gibbons [7], Ryan [8],

This work is licensed under a Creative Commons Attribution-NonCommercial-NoDerivatives 4.0 License. For more information, see https://creativecommons.org/licenses/by-nc-nd/4

This article has been accepted for publication in IEEE Access. This is the author's version which has not been fully edited and
content may change prior to final publication. Citation information: DOI 10.1109/ACCESS.2024.3494042

Montgomery [9] and Stoumbos, Reynolds, and Woodall [10].

In SPC, it is generally assumed that the continuous process variable being measured follows a normal distribution [11]–[13]. This assumption is used to design and evaluate the statistical performance of a control chart [?]. The Shewhart models are frequently utilized for making decisions regarding process performance. However, these methods are not very effective at quickly detecting small changes in monitoring values because they consider data from only the current sample [14]–[16]. To address this limitation, control charts such as EWMA and CUSUM are used [17]. These charts incorporate past sample data to improve the ability to detect small and moderate changes in the studied parameters. To further enhance the performance of time memory-type charts, adaptive approaches are utilized. Adaptive control charts are used when the shift sizes are unknown but are expected to fall within certain intervals [18]. Recent studies have explored the use of memory-type adaptive control charts, such as adaptive EWMA (AEWMA) and adaptive CUSUM (ACUSUM) control charts, which have been shown to be more efficient at detecting shifts of different sizes [19], [20]. Noor et al. [21] proposed an adaptive scheme-based control chart that uses the ranking sampling method to improve the detection of shift sizes. Yi and Qiu [22] suggested another adaptive CUSUM to identify the drift problem in target parameters. Haq and Rizzaq [23] proposed a weighted adaptive scheme for improving the performance of the conventional CUSUM scheme. Adaptive monitoring schemes are highly effective in detecting shifts of different sizes in process parameters, making them versatile for a range of applications. However, owing to the complex computational procedures involved, their practicality in real-time industrial settings may be limited.

The assumption of a normal distribution is commonly used in the design of control charts. However, in many cases, the actual distribution of the study parameters may deviate significantly from normal, which can greatly affect the performance of the control chart [24]. Control charts for nonnormal data offer the advantages of better capturing the complex and diverse nature of real-world data, revealing potential outliers or anomalies and providing a richer understanding of underlying patterns. Numerous authors have investigated the robustness of various Shewhart models and EWMA and CUSUM control charts for monitoring process parameters when the data do not follow a normal distribution [25]–[33]. The CUSUM charts designed for normal processes can result in higher false alarm rates when the data are skewed or have heavy tails [34]–[36]. Therefore, it is important to select an appropriate statistical model for the process to obtain reliable results. Some CUSUM-type charts have been developed for monitoring nonnormal processes, including those that follow exponential, t, Weibull and gamma distributions [18], [37]–[39]. In many cases, the Maxwell distribution provides a reasonable fit for asymmetric datasets [40]–[42]. The Maxwell model is a commonly utilized statistical distribution, especially in the domains of reliability analysis, statistical mechanics and computational chemistry [43]–[46]. The V-control chart, which is based on the Maxwell model, has been suggested as a graphic tool to monitor the square form of the scale parameter of the Maxwell distribution process [47]. The EWMA and CUSUM variants of the V-control chart were developed in previous studies [48], [49]. Another faster scheme, namely, the V_{SQ}-chart for monitoring abrupt changes in the scale parameter under the Maxwell model, was proposed in [50]. Owing to the significant need for tracking subtle variations in the target parameter of Maxwell quality characteristics, Hossain et al. [48] introduced the VCUSUM chart, which was designed for the square quantity of the scale parameter. Nevertheless, in practical applications, there is occasionally a preference to assess the scale parameter of Maxwell distributed data directly rather than its squared quantity. The idea of directly monitoring the Maxwell scale parameter provides the foundation for the V_{SQ}-chart. All the above studies motivated us to design and investigate the potential use of the CUSUM structure in the V_{SQ}-chart. The existing V_{SQ}-chart follows the standard layout of the Shewhart model. The CUSUM structure has advantages over the conventional Shewhart model, especially for detecting smaller changes in the monitoring parameters. To our knowledge, the CUSUM scheme for the V_{SQ}-chart referred to as the MXCUSUM chart has not been designed in the literature.

This study introduces a novel MXCUSUM approach for detecting minor process changes on the basis of the Maxwell model, filling a gap in current research. The proposed chart is designed to efficiently detect minor shifts in the studied parameter. Its distinction from the existing V_{SQ}-chart lies in its enhanced ability to detect smaller shifts in the monitoring process. The primary contributions of this work can be summarized as follows:

- C1 An efficient design for detecting smaller changes in processes following the Maxwell distribution is proposed
- C2 The design parameters and performance indicators of the proposed MXCUSUM are studied via Monte Carlo simulations.
- C3 The practical applicability of the proposed MXCUSUM chart is demonstrated via industrial data.

This research presents a new CUSUM control chart that is specifically tailored for monitoring processes that follow the Maxwell distribution. This chart fills a notable void in current statistical process control techniques.

This work is licensed under a Creative Commons Attribution-NonCommercial-NoDerivatives 4.0 License. For more information, see https://creativecommons.org/licenses/by-nc-nd/4

This article has been accepted for publication in IEEE Access. This is the author's version which has not been fully edited and
content may change prior to final publication. Citation information: DOI 10.1109/ACCESS.2024.3494042

By customizing the CUSUM chart to the specific attributes of the Maxwell process, the authors improve the ability to identify small changes in process parameters (see C1), which is especially advantageous in industries such as carbon fiber manufacturing, where accuracy and excellence are crucial (see C3). Compared with conventional monitoring techniques, the presented chart is more effective, highlighting its ability to accurately detect alterations in both the average and variability of the process, especially when confronted with nonnormal data distributions (see C2). Moreover, the research confirms the practical use of the new CUSUM chart by analyzing real-world data on carbon fiber strength, demonstrating its reliability and effectiveness in a crucial industrial setting (see C3). This application not only strengthens the theoretical breakthroughs discussed in the paper but also highlights the chart's ability to enhance quality control techniques in many sectors.

The paper is structured as follows. Section 2 reviews the theoretical foundation of the proposed chart and introduces the MXCUSUM chart. A thorough performance evaluation of the chart is presented in Section 3. Section 4 provides a comparative analysis of the proposed model. The implementation of the proposed charts is illustrated via a simulated dataset in Section 5. In Section 6, the methodology of the proposed chart is explained via two real datasets. Finally, Section 7 summarizes the key findings and conclusions of the study.

II. PROPOSED CONTROL CHART

In this section, we discuss the concepts of the one-parameter Maxwell model, a general framework of the V_{SQ} chart and the proposed design of the MXCUSUM monitoring scheme for identifying persistent shifts in the scale parameter of the Maxwell process.

An industrial process with an output characteristic that is of interest is considered. We assume for this discussion that the output characteristic is well modeled by the Maxwell distribution with the following model:

$$h(t,\theta) = \sqrt{\frac{2}{\pi}}\left(\frac{t}{\theta^3}\right)^2 e^{-\frac{t^2}{2\theta^2}}; \quad \theta > 0,\, t > 0 \qquad (1)$$

where t are the values of the Maxwell following random variable T and where θ is the scale parameter. The density curves of the Maxwell process are depicted in Figure 1 for different values of the scale parameter. An increase in θ indicates that the density curve of the Maxwell quality becomes symmetric, and a decrease in θ leads to a more right-skewed curve, as shown in Figure 1.

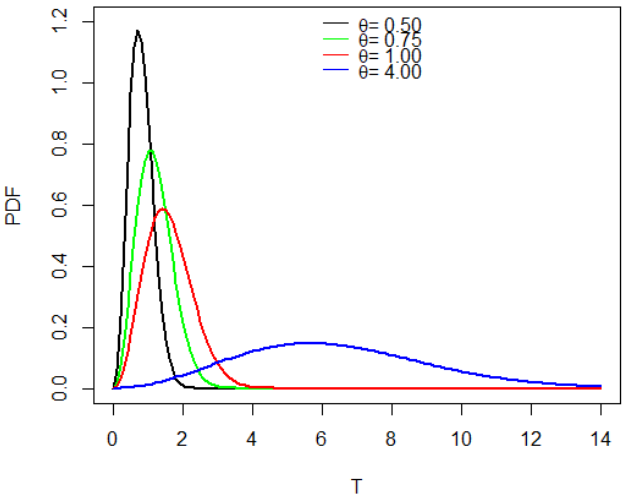

FIGURE 1. Density curves of the Maxwell quality outputs

Numerous production industrial problems yield measures with positively skewed models, such as insurance claims, time to completion of tasks, and component reliability. The Maxwell distribution is a flexible statistical model, particularly in the fields of chemistry, statistical mechanics, the Wiener process, degradation studies and system failure analysis. In industrial settings, the value of the Maxwell parameter is seldom known, and most studies utilize the traditional maximum likelihood (ML) approach. Consider a set of m observations: $w_1, w_2, \ldots, w_m$ are taken as random variables from the Maxwell model. The point estimator of θ using the ML method is given below [51]:

$$\hat{\theta} = \sqrt{\frac{\sum_{i=1}^{m} w_i^2}{3m}} \qquad (2)$$

Referring to Maxwell processes, the V-chart was created by Hossain, Omar, and Riaz [47] to monitor the parameters of the underlying Maxwell process. The proposed methodology of the V-chart is rooted in the basic structure of the Shewhart-type monitoring scheme and is based on the square quantity of the scale parameter. In contrast, the V_{SQ}-chart is another enhanced alternative proposed by Shah et al. [50] for identifying the different shifts in the scale factor of the Maxwell output. The sampling statistic in the V_{SQ}- chart is given by:

$$V_{SQ} = \sqrt{\hat{\theta}^2} \qquad (3)$$

The pivotal quantity of the V_{SQ} chart is given by [50]:

$$V_{SQ} = \frac{\theta}{\sqrt{3m}} U \qquad (4)$$

where $U = \sqrt{\sum_{i=1}^{m} w_i^2}$ follows the chi-distribution with a 3m parameter (details are provided in Appendix A).

This work is licensed under a Creative Commons Attribution-NonCommercial-NoDerivatives 4.0 License. For more information, see https://creativecommons.org/licenses/by-nc-nd/4

This article has been accepted for publication in IEEE Access. This is the author's version which has not been fully edited and
content may change prior to final publication. Citation information: DOI 10.1109/ACCESS.2024.3494042

The shapes of V_{SQ} for different values of the monitoring parameter θ and sample size m are shown in Figure. 2.

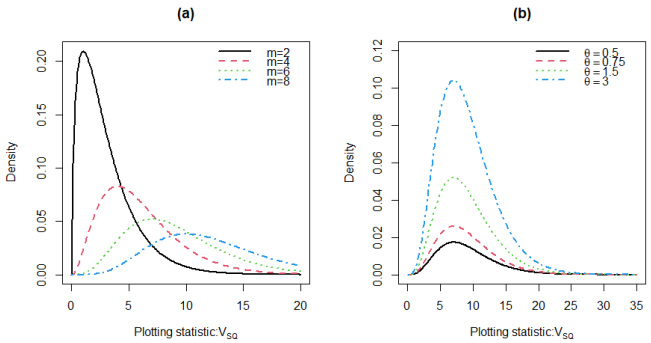

FIGURE 2. The behavior of plotting statistics with respect to (a) a fixed value of θ and varying sample size (m) and (b) a fixed value of sample size (m) and varying θ

The V_{SQ} statistic, as outlined in (4), is influenced by two factors: the sample size and the scale parameter chosen for the Maxwell distribution. The impact of these two factors on the shape of the plotting statistic can be observed in Figure 2. Figure 2 clearly shows the presence of skewness, a characteristic that remains unless the scale parameter and/or sample size are significantly increased. Following practical considerations in the SPC, it is common to choose a sample size that is moderate, typically falling within the range of 1–10. This decision is influenced by the constraints outlined in [8]. The k-sigma limits of the V_{SQ}-chart based on the corresponding sampling distribution of the square root statistic are defined as [50]:

$$\begin{aligned} \mathrm{LCL} &= \theta \mathrm{T_m} - \mathrm{k}\theta\sqrt{1-\mathrm{T_m^2}} \\ \mathrm{UCL} &= \theta \mathrm{T_m} + \mathrm{k}\theta\sqrt{1-\mathrm{T_m^2}} \end{aligned} \tag{5}$$

where k is the quantile of the chi distribution chosen according to the set value of the false alarm rate α and where $\mathrm{T_m} = \sqrt{\frac{2}{3\mathrm{m}}}\frac{\gamma\left(\frac{3\mathrm{m}+1}{2}\right)}{\gamma\left(\frac{3\mathrm{m}}{2}\right)}$ is a function of sample size. Similarly, the probability limits of the V_{SQ}-chart with a known value of θ are given by:

$$\left.\begin{aligned} \mathrm{UPL} &= \frac{\theta}{\sqrt{3\mathrm{m}}}\mathrm{F}^{-1}\left(1-\tfrac{\alpha}{2}\right) = \theta \mathrm{P}_1 \\ \mathrm{LPL} &= \frac{\theta}{\sqrt{3\mathrm{m}}}\mathrm{F}^{-1}\left(\tfrac{\alpha}{2}\right) = \theta \mathrm{P}_2 \end{aligned}\right\} \tag{6}$$

where $\mathrm{P}_1 = \frac{\mathrm{F}^{-1}\left(1-\frac{\alpha}{2}\right)}{\sqrt{3\mathrm{m}}}$, $\mathrm{P}_2 = \frac{\mathrm{F}^{-1}\left(\frac{\alpha}{2}\right)}{\sqrt{3\mathrm{m}}}$ and F^{-1} are the percentile points of the chi distribution (see Appendix A). The V_{SQ}-chart performs better in spotting the moderate to greater changes in the scaling factor of the Maxwell process. The CUSUM framework of the V_{SQ}-chart can be built as follows to further improve the out-control performance of the V_{SQ}-chart under circumstances of smaller to moderate shifts in the examined parameter. Let us draw a rational subgroup of size m from the Maxwell distribution and compute the V_{SQ} statistic given in (3). As the distribution of V_{SQ} is a chi distribution with 3m degrees of freedom, the density function can be expressed as:

$$\mathrm{f}(\mathrm{u}) = \frac{1}{2^{\frac{3}{2}\mathrm{m}}\Gamma\left(\frac{3\mathrm{m}}{2}\right)}\mathrm{u}^{\frac{3\mathrm{m}}{2}-1}\mathrm{e}^{-\frac{\mathrm{u}}{2}}, \qquad \mathrm{m}, \quad \mathrm{u} > 0. \tag{7}$$

By utilizing (4) and the transformation approach, the density function of the V_{SQ} statistics can be written as:

$$\mathrm{f}(\mathrm{v}) = \frac{1}{2^{\frac{\alpha}{2}-1}\Gamma\left(\frac{\alpha}{2}\right)}\left(\frac{\sqrt{\alpha}}{\theta}\right)^{\alpha}\mathrm{v}^{\alpha-1}\mathrm{e}^{-\frac{\mathrm{v}^2\alpha}{2\theta^2}}; \qquad \theta, \mathrm{v} > 0 \tag{8}$$

where $\alpha = 3\mathrm{m}$ and the density $\mathrm{f}(\mathrm{v})$ belong to one exponential family. Since the density function $\mathrm{f}(\mathrm{v})$ is continuous and can be referred to as a special case of the exponential family, it can further be written as:

$$\begin{aligned} \mathrm{f}(\mathrm{v}) = \exp\Bigg\{ &\log\left(\frac{1}{2^{\frac{\alpha}{2}}\Gamma\left(\frac{\alpha}{2}\right)}\right) + \frac{\alpha}{2}\log\alpha - \alpha\log\theta + \\ &+ (\alpha-1)\log\mathrm{v} - \frac{\mathrm{v}^2\alpha}{2\theta^2}\Bigg\} \end{aligned} \tag{9}$$

Let us assume that α is fixed and known in expression (9); then, the reference value of the proposed MX-CUSUM can be computed as:

$$\mathrm{k} = -\frac{\mathrm{A}(\theta_1) - \mathrm{A}(\theta_0)}{\eta(\theta_1) - \eta(\theta_0)} \tag{10}$$

where $\mathrm{A}(\theta)$ and $\eta(\theta)$ are the known components of the exponential family for which we intend to detect shifts in the Maxwell control parameter from θ_0 to θ_1. According to expression (9), the components $\mathrm{A}(\theta)$ and $\eta(\theta)$ and the function of the data can be written as:

$\mathrm{A}(\theta) = -\alpha\log(\theta), \quad \eta(\theta) = -\frac{\alpha}{2}\theta^2, \quad \mathrm{T}(\mathrm{v}) = \mathrm{v}^2.$

Thus,

$$\left.\begin{aligned} \mathrm{A}(\theta_1) - \mathrm{A}(\theta_0) &= \alpha\log\left(\frac{\theta_0}{\theta_1}\right) \\ \eta(\theta_1) - \eta(\theta_0) &= \frac{\alpha}{2}\left(\frac{1}{{\theta_0}^2} - \frac{1}{{\theta_1}^2}\right) \end{aligned}\right\} \tag{11}$$

Using (11) in (10) leads to the following expression:

$$\mathrm{k} = -\frac{2\log\left(\frac{\theta_0}{\theta_1}\right)}{\left(\frac{1}{{\theta_0}^2} - \frac{1}{{\theta_1}^2}\right)} \tag{12}$$

Note that by tuning a CUSUM for a normal distribution, the reference value k is typically set at the midpoint between the IC and OC means. However, in the case of a Maxwell distribution, the reference value k may not be exactly at this midpoint but may be obtained through expression (12). The value of k is zero for the in-control (IC) state process, and its value depends upon the amount of shift, i.e., a value specified for the out-of-control (OC) state. For different values of the shift in the monitoring parameter θ, the computed values of k are given in Table 1.

This work is licensed under a Creative Commons Attribution-NonCommercial-NoDerivatives 4.0 License. For more information, see https://creativecommons.org/licenses/by-nc-nd/4

This article has been accepted for publication in IEEE Access. This is the author's version which has not been fully edited and
content may change prior to final publication. Citation information: DOI 10.1109/ACCESS.2024.3494042

TABLE 1. The computation of reference value *k* at different shift size

Increased in monitoring parameter	Shift size	k
0%	1	0
10%	1.1	0.62
15%	1.15	0.64
20%	1.2	0.67
25%	1.25	0.7
30%	1.3	0.72
35%	1.35	0.75
40%	1.4	0.77
50%	1.5	0.82
80%	1.8	0.96
100%	2	1.04

To detect a rise in the scale parameter of the Maxwell distribution from the IC value θ_0 to a larger value θ_1. Then, the charting statistic of the MXCUSUM monitoring scheme can be established as:

$$M_n{}^{+} = \max\left(0,\ M_{n-1}{}^{+} + v_n^2 - k^{+}\right) \qquad (13)$$

where $M_0{}^{+} = 0$ and the value of k can be computed from the expression given in (12). The decision interval L^{+} is the only factor remaining in designing the MXCUSUM chart. The value of L^{+} is chosen such that the desired IC value of the average run length (ARL_0) is achieved. To compute this value of L^{+}, a program written in R is utilized. The computed values of L^{+} for the Maxwell process across the different sample sizes are shown in Table 2 and Table 3.

TABLE 2. The computation of value *L* for different shifts at $ARL_0 = 370$

k	Subgroup Size			
	m=1	m=3	m=6	m=10
0	207.714	207.714	207.714	207.714
0.62	4.855	2.115	1.211	0.788
0.67	3.766	1.521	0.828	0.516
0.72	3.167	1.226	0.64	0.386
0.77	2.77	1.031	0.521	0.3
0.96	2.065	0.668	0.274	0.095
1.04	1.87	0.5603	0.1846	0.011

TABLE 3. The computation of value *L* for different shifts at $ARL_0 = 200$

k	Subgroup Size			
	m=1	m=3	m=6	m=10
0	112.06	112.06	112.21	112.21
0.62	3.872	1.741	1.017	0.665
0.67	3.091	1.281	0.701	0.437
0.72	2.643	1.033	0.543	0.326
0.77	2.344	0.876	0.443	0.252
0.96	1.715	0.542	0.204	0.045
1.04	1.557	0.446	0.121	0.022

Thus, the MXCUSUM monitoring scheme will signal if $M_n{}^{+} > L^{+}$, which completely specifies the MXCUSUM chart. If our intention is toward a downward shift in the scale parameter, then the following monitoring statistics can be used:

$$M_n{}^{-} = \min\left(0,\ M_{n-1}{}^{-} + v_n^2 - k^{-}\right) \qquad (14)$$

where $M_0{}^{-} = 0$, k^{-} is computed from (12), and the downward MXCUSUM chart will signal if $M_n{}^{-} < L^{-}$. Owing to our aim for detecting an increasingly smaller shift in the scale parameter of the Maxwell quality characteristic, the one-sided MXCUSUM charts established in (12) and (13) are utilized in this work.

III. PERFORMANCE ASSESSMENT

The performance of the proposed chart is primarily determined by the average run length (ARL) approach, which is the most prevalent and effective method. The computation of the ARL can be accomplished through the use of integral equations, discrete approximations to the integral equations via Markov chains, and simulation schemes. Given the advanced computing facilities available today, the simulation approach is more appropriate and accurate than the approximation formulas are. As a result, a Monte Carlo program written in R software was employed to compute ARL in this study. This approach is highly adaptable to various situations and is generally more precise than other numerical algorithms based on Monte Carlo simulations that have been developed in previous studies. We have identified the optimal statistic and reference value k for the proposed MXCUSUM scheme in (10) and (13), respectively. Two parameters, L and k, must be chosen before the chart can be used for process monitoring. The values of L and k clearly have a significant effect on the performance of the proposed chart. Given values of h and k, we can compute the in-control ARL (ARL_0) and out-of-control ARL (ARL_1) of the MXCUSUM chart via the algorithm described by the pseudocode below: Let K be the number of replicated simulations. In our case, we selected K = 100000. For any ith run, compute the run length RL (i) as follows:
An independent random sample of a particular size m is generated from the Maxwell model with scale parameter θ.
Compute the value $M_n{}^{+}$ via (13).
If $M_n{}^{+} > L^{+}$ is satisfied, set RL (i) = m and stop the loop; otherwise, let m = m + 1 and continue the loop.
The ARL can be estimated by calculating the simple average of the K run length values {RL(i), i = 1, 2, . . . , K }.
The pseudocode (see Appendix A) shown above requires that observations at different time points in a simulation be independent of each other. Additionally, we focused primarily on computing the one-sided MXCUSUM chart. This is especially important in situations where an upward shift is more critical than a downward shift, as an increase in variation is typically more detrimental than a decrease in variation when monitoring a process.

This work is licensed under a Creative Commons Attribution-NonCommercial-NoDerivatives 4.0 License. For more information, see https://creativecommons.org/licenses/by-nc-nd/4

This article has been accepted for publication in IEEE Access. This is the author's version which has not been fully edited and
content may change prior to final publication. Citation information: DOI 10.1109/ACCESS.2024.3494042

The ARL values for the MXCUSUM chart, as well as the standard deviation of the run length distribution (SDRL) and median run length (MRL), are presented in Table 4 and Table 5 for different ARL_0.

TABLE 4. Performance of the MXCUSUM chart across the various subgroup sizes

Shifting	$ARL_0 = 370$								
	m=3			m=6			m=10		
parameter	ARL	MRL	SDRL	ARL	MRL	SDRL	ARL	MRL	SDRL
1	369.43	370	9.07	369.92	370	6.43	370.07	370	4.93
1.1	28.8	23	20.09	18.15	15	11.98	12.55	10	7.97
1.2	11.09	9	7.23	6.63	6	4.07	4.56	4	2.62
1.3	6.21	5	3.94	3.7	3	2.15	2.52	2	1.42
1.4	4.14	4	2.58	2.46	2	1.41	1.72	1	0.91
1.8	1.73	1	0.97	1.18	1	0.45	1.02	1	0.17
2	1.40	1	0.68	1.06	1	0.25	1	1	0.07

TABLE 5. Performance of the MXCUSUM chart across the various subgroup sizes

Shifting	$ARL_0 = 200$								
	m=3			m=6			m=10		
parameter	ARL	MRL	SDRL	ARL	MRL	SDRL	ARL	MRL	SDRL
1	199.91	200	6.61	200.06	200	4.64	200.03	200	3.61
1.1	23.15	19	16.65	15.14	12	10.46	10.61	9	6.99
1.2	9.44	8	6.33	5.75	5	3.59	3.99	3	2.35
1.3	5.4	5	3.51	3.29	3	1.97	2.28	2	1.31
1.4	3.68	3	2.36	2.25	2	1.31	1.58	1	0.82
1.8	1.61	1	0.88	1.14	1	0.39	1.02	1	0.14
2	1.33	1	0.63	1.05	1	0.22	1	1	0.07

Table 4 displays the various characteristics of the run length for different sample sizes and shifts. It is apparent from Table 4 that the ARL decreases as the shift increases. For the IC state, the value of ARL_0 is near the nominal value of 370, which suggests that when no significant shift occurs, the first signal is observed on average at every 370th plotted point. Moreover, as anticipated, the SDRL and MRL values decrease as the shift increases. The collective outcomes presented in Table 4 suggest that the MXCUSUM is highly sensitive and is the preferred method for detecting smaller shifts in the parameter being studied. A similar trend is also shown in Table 5.

IV. SIMULATION ANALYSES

In this particular section, we aim to showcase the practical application of the proposed chart using simulated data to investigate the quality of a specific part in a manufacturing process. Under normal operating conditions, the quality characteristic of this part is assumed to follow a Maxwell distribution with a scale parameter of 0.75. To carry out the study, we randomly selected 10 sets of 3 observations from the stable process and another 10 sets of 3 observations from the process after introducing a 10% and 20% upward shift in the target parameter. As a result, new Maxwell processes were generated with scale parameters of 0.83 and 0.90. The data used for analysis were collected at 20 consecutive time points from the production process, with the initial distribution of the process following a Maxwell distribution with a scale parameter of 0.75. At the 11th time point, the process underwent scale shifts of 1.10 and 1.20, respectively. To visually represent the shift increases of 10% and 20% in the studied parameter, we present the conventional V_{SQ} chart and the proposed MXCUSUM control chart in Figure 3 and Figure 4.

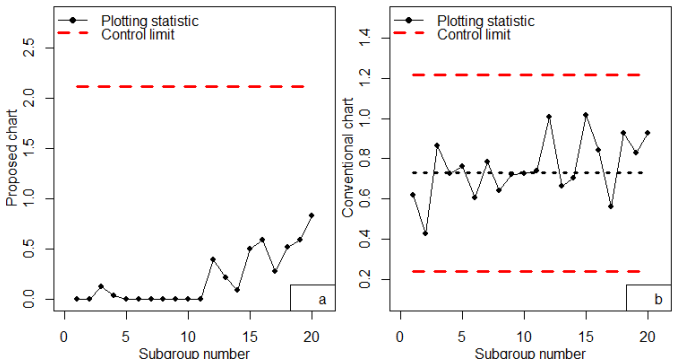

FIGURE 3. Control charts based on simulated data with a 10% increase in the scale parameter: (a) proposed chart and (b) existing chart

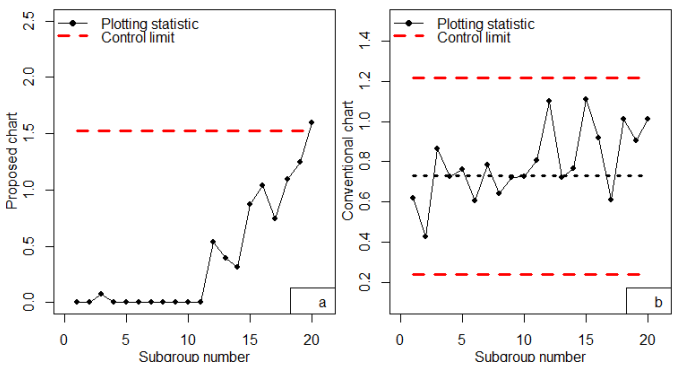

FIGURE 4. Control charts based on simulated data with a 20% increase in the scale parameter: (a) proposed chart and (b) existing chart

The provided information pertains to Figure 3(b), which displays the V_{SQ} chart developed using 20 samples and control limits computed via formulas in (5), with setup values of $ARL_0 = 370$ and $m = 3$. Analysis of the traditional chart indicated process stability, and no abnormalities were observed in the 20 consecutive samples. However, a careful examination of Figure 3(a) reveals that a minor shift occurred during the 11th time point that was undetected by the existing chart. Conversely, the proposed chart, constructed using all 20 samples and control limits computed by the formulas in (13), clearly depicts an upward trend that initiates at the 11th sample. Similarly, Figure 4 also illustrates that the proposed chart is capable of detecting smaller shifts quickly.

V. COMPARATIVE ANALYSES

Here, we look at how the MXCUSUM chart stacks up against its closest competition, the V_{SQ} chart, in terms

This work is licensed under a Creative Commons Attribution-NonCommercial-NoDerivatives 4.0 License. For more information, see https://creativecommons.org/licenses/by-nc-nd/4

This article has been accepted for publication in IEEE Access. This is the author's version which has not been fully edited and
content may change prior to final publication. Citation information: DOI 10.1109/ACCESS.2024.3494042

of power. Correct indications of changes in the process distribution might be provided by the control charts. If the process becomes OC at some point in the future, the relevant control chart alerts us of the change after an appropriate elapsed time. This is the so-called power of the test in the context of testing hypotheses; it is indicated by $1-\beta$, where β is the likelihood of making a Type-II mistake. This is the likelihood of truly rejecting the null hypothesis of the IC process. The type-I error is often fixed at a predetermined level and is minimized by combining the control chart technique with hypothesis testing. This ultimately improved the efficacy of the investigated control treatment. Fixing the IC ARL and minimizing the OC ARL is a tactic not unlike that employed in a control chart setting. Smaller values of β indicate rapid OC indication, and a control chart has superior performance. In other words, a control chart with greater power is deemed superior in a particular circumstance. Our process is considered stable with a scale value of 0.75. The power curves of the MXCUSUM chart and V_{SQ} chart describe their capacity to detect changes in process parameters. The algorithm specified in Section 3 has been employed to generate power curves for the proposed chart. As illustrated in Figure 5, these power curves are generated for various sample sizes at a constant ARL_0 equal to 370.

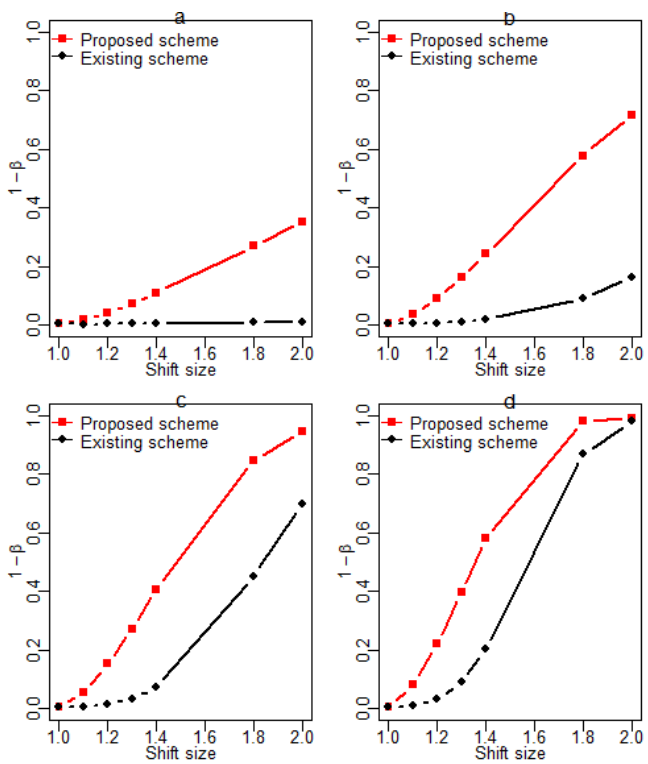

FIGURE 5. Comparison of the proposed chart with existing charts for sample sizes of (a) $m = 1$, (b) $m = 3$, (c) $m = 6$, and (d) $m = 10$

Figure 5 displays the power curves for the proposed chart and the typical chart. Figure 5 demonstrates that the suggested chart is extremely successful in detecting changes of varying magnitudes across sample sizes. For example, if the scale parameter changes from 0.75 to (0.82, 0.87, and 0.92), the capacity of the suggested chart to identify this shift is (0.0347, 0.0902, and 0.1610), which is greater than the comparable probabilities (0.0030, 0.0056, 0.0101) of the V_{SQ} chart with a sample size m equal to 3. This gap in power increases as the sample size increases; it is greater for larger sample sizes. Thus, the suggested graph in 5 demonstrates that the MXCUSUM chart is superior to the V_{SQ}chart for varying shifts in the study parameter.

VI. REAL DATA LILUSTRATION

In this section, we present our proposed chart using a real dataset. To provide more clarity on the proposed design and computational procedure, a comprehensive block diagram is shown in Figure 6.

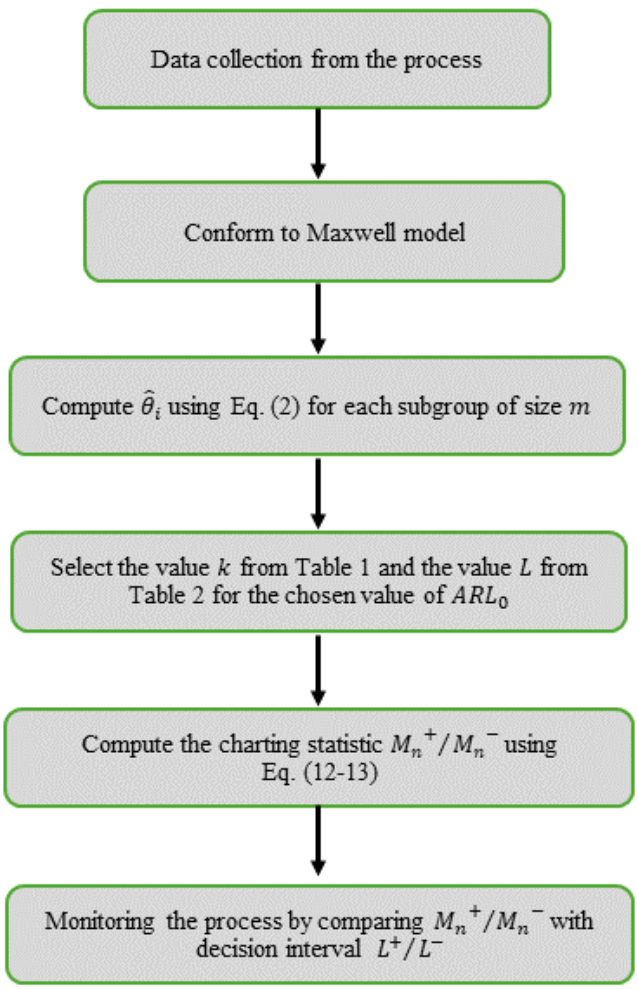

FIGURE 6. Stepwise block diagram of the proposed scheme

This work is licensed under a Creative Commons Attribution-NonCommercial-NoDerivatives 4.0 License. For more information, see https://creativecommons.org/licenses/by-nc-nd/4

This article has been accepted for publication in IEEE Access. This is the author's version which has not been fully edited and
content may change prior to final publication. Citation information: DOI 10.1109/ACCESS.2024.3494042



FIGURE 7. An overview of the carbon fiber production process[52]

A real dataset on the breaking strength of carbon fibers is employed for the construction of the MX-CUSUM chart. The manufacturing process for the carbon fiber material is depicted in Figure 7, taken from the secondary source [52] for visual representation. There are various methods used to test the strength of carbon fibers to guarantee their quality and performance. Testing the strength of carbon fibers is crucial for reasons such as selecting materials, optimizing performance, ensuring quality, and maintaining safety standards. Manufacturers can confirm the quality of their products and maintain consistent material properties by conducting thorough strength tests. The data used in this study show the strength values in GPA (gigapascal) for both single carbon fibers and impregnated tows of 1000 carbon fibers. Single fibers underwent tension testing at gauge lengths of 1, 10, 20, and 50 mm. For illustration purposes, we utilized the dataset resulting from the 20 mm gauge length test. The dataset consists of 60 observations that were subjected to tension testing with a gauge length of 20 mm. The data, previously employed in multiple studies, serve as an illustration of the practical uses of recently introduced distributions and their significance in reliability studies [4], [53]–[55]. The dataset's inception is credited to the research conducted by [56]. The Maxwell distribution is widely used in reliability studies to predict failure times and in statistical mechanics to depict random particle speeds. Motivated by the analogous backgrounds depicted, there is significant interest in exploring the suitability of the Maxwell distribution as an alternative to carbon strength data. To evaluate whether the carbon strength measurements followed a Maxwell distribution, we originally used probability plotting as a graphical tool. However, this process was complicated and could not be easily performed via the built-in fitdistplus library in R software. As a result, we developed a custom function to assist in fitting the Maxwell distribution to the actual dataset. Figure 8 displays the fitting plots of the Maxwell model, which were generated via this custom function.

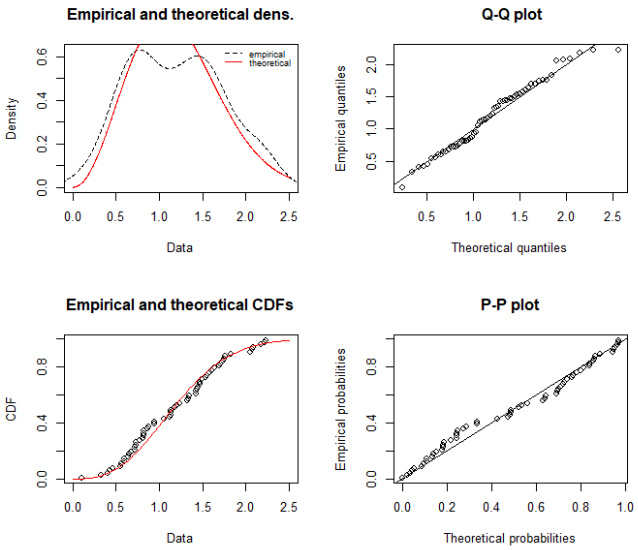

FIGURE 8. Probability plots depicting the carbon strength data

Under the Maxwell model, the solid lines in Figure 8 are used to indicate the best-fit line. Figure 8 shows that these straight lines successfully capture all of the depicted points, suggesting that the Maxwell model offers a plausible representation of the dataset. A study conducted by Shah et al. [50] confirmed that the data follow a Maxwell distribution, with a scaling parameter of 1.07. The validation of the data's conformity to the Maxwell distribution is further substantiated by earlier research conducted by [57]. The original dataset could not be directly fitted to the Maxwell model in the initial attempt. Nevertheless, a suitable fit was reached by modifying the starting point of the dataset, accomplished by subtracting 1.8 from each individual data value. Figure 8 shows that the carbon strength data are skewed to the right. This suggests that potential underlying models such as the Weibull distribution, exponential distribution, gamma distribution, or Maxwell model could be suitable for analysis. Table 6 displays the results of various goodness-of-fit evaluations, including the Kolmogorov–Smirnov (KS), Akaike information criterion (AIC), and Bayesian information criterion (BIC), used to identify the optimal probability distribution for the carbon fiber data. The numerical results in Table 6 indicate that the Maxwell model has excellent AIC and BIC values, although its p value is slightly below the conventional threshold of 0.05 compared with the Weibull model. The Weibull model may be considered the best fit on the basis solely of the p value. Typically, a single model is chosen as the best fit for data generation, but there are instances where multiple models could be equally viable options for a dataset. Importantly, the Maxwell model

This work is licensed under a Creative Commons Attribution-NonCommercial-NoDerivatives 4.0 License. For more information, see https://creativecommons.org/licenses/by-nc-nd/4

This article has been accepted for publication in IEEE Access. This is the author's version which has not been fully edited and
content may change prior to final publication. Citation information: DOI 10.1109/ACCESS.2024.3494042

shows strong performance in terms of other goodness-of-fit measures. Additionally, the basic probability plots in Figure 8 also reflect the suitability of the Maxwell model for analyzing carbon strength data. The stress strength dataset, which originally consisted of 63 observations as described in reference [57], was subsequently modified. The dataset was adjusted by excluding the last three values to ensure an equal distribution of subgroups. This resulted in a dataset of 60 values that were divided into 12 subgroups, each with five observations, as explained in reference [50]. The dataset has been applied to create the MXCUSUM chart for monitoring the Maxwell scale parameter. For every subgroup, the estimate $\hat{\theta}_i$ of the scale parameter is calculated via (2). We illustrate the application of this procedure with a real dataset as an example. An ARL_0 of 370 is our goal, assuming that we want to identify a scale shift from 1.07 to a different value, such as 1.34, which indicates a 25% increase in the recording parameter. What specifications should be considered when designing our MXCUSUM scheme? The only remaining parameter is L, which is the value of the decision interval. We use our simulation program from Section 2 to ascertain this value. The program output yields L = 1.77, and consequently, the designed parameters for the proposed scheme are fully specified as follows:σ_0 = 1.07, m = 5, k = 1.42 and L = 1.77. Similarly, the corresponding design parameters of the MXCUSUM chart for a 15% increase in σ_0 with a sample size of 5 are k = 1.32 and L = 2.38. These parameters are subsequently utilized to simulate 10 observations, incorporating upward shifts of 1.15 and 1.25. Consequently, 22 observations are created for process monitoring, with the first 12 reflecting IC conditions and the following 10 simulated under OC scenarios with 15% and 25% increases in the IC value of σ_0. The findings are shown in Figure 9.

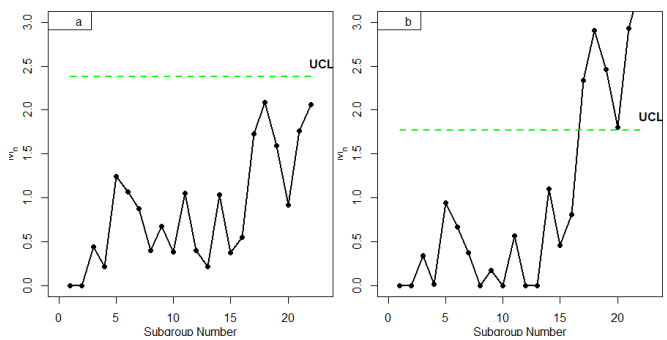

FIGURE 9. Strength data monitoring via the MXCUSUM scheme

Figure 9 shows that the MXCUSUM responds quickly to OC conditions, with an increasing trend after the twelfth observation. Figure 9(a) depicts the identification of an OC situation for a 15% increase in the study parameter, whereas Figure 9(b) depicts an out-of-control scenario for a 25% increase.

TABLE 6. Distribution fitting results for the carbon strength data

Model	Estimated parameter(s)	AIC	BIC	KS-statistic	P-value
Maxwell	0.748	94.45	96.54	0.178	0.0421
Exponential	0.843	142.36	144.45	8.28	0.0001
Weibull	(2.41, 1.33)	94.91	99.1	0.089	0.717
Gamma	(4.10, 3.46)	99.52	103.71	9.4153	0.0001

TABLE 7. Distribution fitting results for the failure times data

Model	Estimated parameter(s)	AIC	BIC	KS-statistic	P-value
Maxwell	1777.6	542.02	543.48	0.149	0.471
Exponential	0.0003	576.03	577.50	1.000	0.000
Weibull	(0.76, 1134.11)	612.92	615.85	0.664	0.000
Gamma	(16.65, 0.01)	590.24	593.17	0.263	0.0195

As a second real-world example, we applied the MXCUSUM chart to the failure times (in hours) of a vertical boring machine, which was originally collected in [44] and subsequently used in [47]–[49] for Maxwell processes in the SPC literature. The Maxwell distribution was found to be a perfect fit for the failure time data, as noted in [47]. To further confirm the suitability of the Maxwell model, Table 7 presents the results from various goodness-of-fit tests. The numerical results in Table 7 suggest that the Maxwell model provides a better fit for the underlying data. The original data consists of the following 32 values [47]:
2937,4020,2802, 2816,2136, 4359,3886,3685, 1781,2655, 3158, 2296,3705,3811,376,2380,4339, 4155, 2172,2076,2848, 808,1701,2672,1976,3632, 1700,4351,3575,4291,3802,1596.
By implementing the proposed chart, the data were divided into 8 groups, each containing 4 observations, as given in Table 6 of the source [47]. Assuming the same data distribution, we estimated the scale parameter of the Maxwell distribution as $\hat{\theta}$ = 1763.13, which is the average value of the $\hat{\theta}_i$ values of 8 subgroups computed on the basis of the expression outlined in (2). To identify a scale shift from 1763.13 to a new value, such as 2115.60 (indicating a 20% increase in the recording parameter), the 20% increase in the scale parameter yields k = 3710536, which is calculated from (12). Using our simulation program from the Appendix, we find the decision interval to be L = 6526367 for m = 4, k = 3710536 and ARL_0 = 370. To assess the effectiveness of the proposed MXEWMA chart in detecting small changes in a real-world data application, eight new values were randomly selected from the Maxwell distribution with the shifted scale parameter θ = 2115.60. The proposed chart, which is based on all 16 observations, is shown in Figure 10, where the first 8 samples represent the IC scenario, and the following 8 samples reflect the shift process.

This work is licensed under a Creative Commons Attribution-NonCommercial-NoDerivatives 4.0 License. For more information, see https://creativecommons.org/licenses/by-nc-nd/4

This article has been accepted for publication in IEEE Access. This is the author's version which has not been fully edited and
content may change prior to final publication. Citation information: DOI 10.1109/ACCESS.2024.3494042

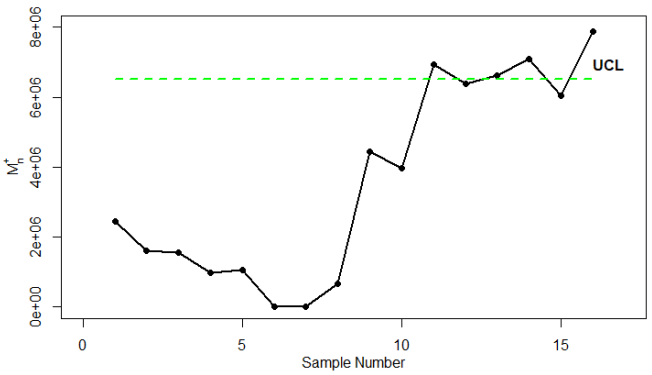

FIGURE 10. **Failure time monitoring via the MXCUSUM control chart**

The chart in Figure 10 reveals an upward trend in the data after the 8th sample, indicating that the process has shifted to the OC state. This again emphasizes the chart's ability to detect even small changes in the scale parameter of the Maxwell data-generating process. .

VII. SUMMARY AND CONCLUSION

This work constructs the MXCUSUM scheme, an extension of the V_{SQ} chart for tracking smaller changes in the process that follows the Maxwell distribution. Compared with the V_{SQ} chart, the MXCUSUM chart has been demonstrated to be successful in identifying smaller shift sizes. The run length properties of the proposed chart were evaluated via Monte Carlo simulations, which indicated that the ARL and SDRL of the MXCUSUM chart are significantly lower for detecting small shifts, thereby confirming its higher sensitivity. by demonstrating higher power across different small shift sizes in the target parameter. According to the study's findings, a process that follows the Maxwell distribution can be monitored for small changes via an MXCUSUM chart as a diagnostic tool. To demonstrate the practical application of the MXUSUM chart, example showcasing strength data are provided. The analysis of real data further confirmed that the MXCUSUM chart is superior in detecting even subtle changes in the scale parameter of the Maxwell process.

The scope of the current study may also be extended to design a more robust structure under the Tukey control chart framework for effectively monitoring the Maxwell data generation process. Additionally, enhancing the MXCUSUM approach by integrating estimated parameters into the design can further improve process monitoring capabilities.

ACKNOWLEDGMENTS

This work has been implemented by the TKP2021-NVA-10 project with support provided by the Ministry of Culture and Innovation of Hungary from the National Research, Development and Innovation Fund, financed under the 2021 Thematic Excellence Programme funding scheme.

APPENDIX A

The V_{SQ} statistic follows a chi-square distribution with 3m df. The proof can be established as follows:

Theorem 1: Let the random variable T follow a Maxwell model with parameter θ; then, the transformation $W = \frac{T^2}{\theta^2}$ conforms to the gamma model with parameters $\frac{3}{2}$ and 2.

Proof. If the random variable T follows a Maxwell distribution with a scaling factor of θ, then the pdf is expressed as:

$$f(t) = \sqrt{\left(\frac{2}{\pi}\right)}\theta^{-3}t^2e^{-\frac{t^2}{2\theta^2}}; \quad t \geq 0, \quad \theta > 0. \tag{A.1}$$

The transformation $W = \frac{T^2}{\theta^2}$ is a one-to-one transformation from $\Omega = \{t\,|t > 0\}$ to $\vartheta = \{w\,|w > 0\}$, with an inverse solution of $w = \frac{t^2}{\theta^2}$ given by:

$$f(w) = \sqrt{\left(\frac{2}{\pi}\right)}\theta^{-3}(\theta^2 w)e^{-\frac{w}{2}} \times \left|\frac{\theta}{2\sqrt{w}}\right| \tag{A.2}$$

Consequently,

$$f(w) = \frac{1}{2^{\frac{3}{2}}\Gamma\left(\frac{3}{2}\right)}w^{\frac{3}{2}-1}e^{-\frac{w}{2}}, \quad w > 0 \tag{A.3}$$

Hence, $W \sim G\left(\frac{3}{2}, 2\right)$. The following is a useful corollary to Theorem 1.

Corollary 1: If $W_1, \ W_2, \ldots W_m,$ are iid gamma distributed random samples with parameters $\frac{3}{2}$ and 2, respectively, then $\sum_{j=1}^{m} W_j \sim G\left(\frac{3}{2}m, 2\right)$.

where $W_j = \frac{T^2}{\theta^2}$, $j = 1, 2, \ldots, m$

Proof. Since each $W_j \sim G\left(\frac{3}{2}, 2\right)$ With the iid property, using the reproductive property of the gamma distribution, we can write: $\sum_{j=1}^{m} W_j \sim G\left(\frac{3}{2}m, 2\right)$, hence proved.

Theorem 2: If $\sum_{j=1}^{m} W_j \sim G\left(\frac{3}{2}m, 2\right)$, then one-one transformation, $U = \sqrt{\sum_{j=1}^{m} W_j}$ follows a chi-distribution with a parameter of 3 m.

Proof. Since $Y = \sum_{j=1}^{m} W_j \sim G\left(\frac{3}{2}m, 2\right)$

This yields:

$$f(z) = \frac{1}{2^{\frac{3}{2}}\Gamma\left(\frac{3}{2}\right)}w^{\frac{3}{2}-1}e^{-\frac{w}{2}}, \quad w > 0 \tag{A.4}$$

$U = \sqrt{Y}$ is a one-to-one transformation from $\Omega = \{y\,|y > 0\}$ to $\vartheta = \{u\,|u > 0\}$ with an inverse solution $y = u^2$.

Therefore, the pdf of the new random variable is given by:

$$f(u) = \frac{1}{2^{\frac{3}{2}m}\,\Gamma\left(\frac{3m}{2}\right)}(u^2)^{\frac{3m}{2}-1}e^{-\frac{u^2}{2}} \times 2u \tag{A.5}$$

This work is licensed under a Creative Commons Attribution-NonCommercial-NoDerivatives 4.0 License. For more information, see https://creativecommons.org/licenses/by-nc-nd/4

This article has been accepted for publication in IEEE Access. This is the author's version which has not been fully edited and
content may change prior to final publication. Citation information: DOI 10.1109/ACCESS.2024.3494042

Simplification (A.5) yields:

$$\mathrm{f}(\mathrm{u}) = \frac{1}{2^{\frac{3\mathrm{m}}{2}-1}\,\Gamma\left(\frac{3\mathrm{m}}{2}\right)}\mathrm{u}^{3\mathrm{m}-1}\mathrm{e}^{-\frac{\mathrm{u}^2}{2}};\ \mathrm{u}>0 \tag{A.6}$$

which conforms to the pdf of the random variable U is indeed a chi-distribution with the 3m parameter. Thus, the mean and variance of U can easily be established. Moreover, the $\mathrm{V_{SQ}}$ statistic can be written as:

$\mathrm{V_{SQ}} = \sqrt{\frac{\sum_{\mathrm{i}=1}^{\mathrm{m}} \mathrm{w_i}^2}{\sigma^2}} \times \frac{\sqrt{3\mathrm{m}}}{\sqrt{3\mathrm{m}}} = \frac{\theta}{\sqrt{3\mathrm{m}}}\mathrm{U}$ Thus, the mean and variance of $\mathrm{V_{SQ}}$ can easily be established to develop k sigma limits, whereas the probability limits can be established by using the percentile function of the chi-square distribution as:

$$\mathrm{F}(\mathrm{u}) = \alpha \tag{A.7}$$

where α is the probability of a false alarm and F is the CDF of the chi distribution. Consequently, further simplification of (A.7) yields:

$$\mathrm{V_{SQ}} = \frac{\theta}{\sqrt{3\mathrm{m}}}\mathrm{F}^{-1}(\alpha) \tag{A.8}$$

Thus, $\mathrm{F}^{-1}\left(1-\frac{\alpha}{2}\right)$ and $\mathrm{F}^{-1}\left(\frac{\alpha}{2}\right)$ are the percentile points of the chi distribution used in the probability limits. A flowchart showing the algorithm for computing the run length distribution characteristics

Algorithm 1 ARL0/ARL1 calculation

Input: k, L, m
Output: AARL0
Set random seed to 100
$\sigma \leftarrow \delta \times 0.75$ ▷ $\delta = 1$ for in-control process
$\mathrm{K} \leftarrow 100000$ ▷ Number of replicated simulations
$\mathrm{N} \leftarrow 4000$ ▷ Longest length of the observation sequence
$\mathrm{AARL0} \leftarrow 0$ ▷ Actual ARL0 value
$\mathrm{num} \leftarrow 0$ ▷ Count of simulations with OC signals
for j ← 1 to K do
  $\mathrm{x} \leftarrow$ array of zeros of length N ▷ Original observation sequence
  cn ← array of zeros of length N ▷ MXCUSUM charting statistic
  $\mathrm{x}[1] \leftarrow \left(\frac{\sigma}{\sqrt{3\mathrm{m}}}\right) \times \mathrm{rchi}(1, 3\mathrm{m})$ ▷ Generate sample from desired statistic
  $\mathrm{cn}[1] \leftarrow \max(0, \mathrm{x}[1]^2 - \mathrm{k})$
  if $\mathrm{cn}[1] > \mathrm{L}$ then
    $\mathrm{AARL0} \leftarrow \mathrm{AARL0} + 1$
    $\mathrm{num} \leftarrow \mathrm{num} + 1$
    continueing
  end if
  for i ← 2 to N do
    $\mathrm{x}[\mathrm{i}] \leftarrow \left(\frac{\sigma}{\sqrt{3\mathrm{m}}}\right) \times \mathrm{rchi}(1, 3\mathrm{m})$
    $\mathrm{cn}[\mathrm{i}] \leftarrow \max(0, \mathrm{cn}[\mathrm{i}-1] + \mathrm{x}[\mathrm{i}]^2 - \mathrm{k})$
    if $\mathrm{cn}[\mathrm{i}] > \mathrm{L}$ then
      $\mathrm{AARL0} \leftarrow \mathrm{AARL0} + \mathrm{i}$
      $\mathrm{num} \leftarrow \mathrm{num} + 1$
      break
    end if
  end for
end for
$\mathrm{SDRL} \leftarrow \mathrm{sd}(\mathrm{AARL0})$
$\mathrm{MRL} \leftarrow \mathrm{median}(\mathrm{AARL0})$
$\mathrm{AARL0} \leftarrow \frac{\mathrm{AARL0}}{\mathrm{num}}$
$\alpha \leftarrow \frac{1}{\mathrm{AARL0}}$ (In the case where $\delta = 1$, provide power for the IC process)
Power $\leftarrow \frac{1}{\mathrm{AARL0}}$ (In the case where $\delta > 1$, provide power for the OC process)

REFERENCES

[1] Fuad S Alduais and Zahid Khan. Ewma control chart for rayleigh process with engineering applications. IEEE Access, 11:10196–10206, 2023.
[2] Sajid Ali and Muhammad Riaz. Cumulative quantity control chart for the mixture of inverse rayleigh process. Computers & Industrial Engineering, 73:11–20, 2014.
[3] Robert G Aykroyd, Víctor Leiva, and Fabrizio Ruggeri. Recent developments of control charts, identification of big data sources and future trends of current research. Technological Forecasting and Social Change, 144:221–232, 2019.
[4] Dadasaheb G Godase, Shashibhushan B Mahadik, and Athanasios C Rakitzis. The sprt control charts for the maxwell distribution. Quality and Reliability Engineering International, 38(4):1713–1728, 2022.
[5] Shahid Hussain, Xiaoguang Wang, Shabbir Ahmad, and Muhammad Riaz. On a class of mixed ewma-cusum median control charts for process monitoring. Quality and Reliability Engineering International, 36(3):910–946, 2020.
[6] Sajid Ali, Maria Asghar, and Ismail Shah. Generalized linear model based gamma control chart. Quality and Reliability Engineering International, 40(1):699–711, 2024.
[7] Robert D Gibbons, Dulal K Bhaumik, and Subhash Aryal. Statistical methods for groundwater monitoring. John Wiley & Sons, 2009.
[8] Thomas P Ryan. Statistical methods for quality improvement. John Wiley & Sons, 2011.
[9] Douglas C Montgomery. Introduction to statistical quality control. John wiley & sons, 2019.
[10] Zachary G Stoumbos, Marion R Reynolds Jr, and William H Woodall. Ch. 13. control chart schemes for monitoring the mean and variance of processes subject to sustained shifts and drifts. Handbook of Statistics, 22:553–571, 2003.
[11] Leo CE Huberts, Marit Schoonhoven, Rob Goedhart, Mandla D Diko, and Ronald JMM Does. The performance of control charts for large non-normally distributed datasets. Quality and Reliability Engineering International, 34(6):979–996, 2018.
[12] Nabeel Ahmed, Sajid Ali, and Ismail Shah. Control charts for monitoring mean of generalized exponential distribution with type-i censoring. Quality and Reliability Engineering International, 38(1):592–614, 2022.
[13] Hafiz Zafar Nazir, Tahir Hussain, Zameer Abbas, Noureen Akhtar, Muhammad Abid, and Muhammad Riaz. On developing robust adaptive approaches for monitoring location of non-normal environments. Quality and Reliability Engineering International, 38(1):326–342, 2022.
[14] Inez M Zwetsloot, Marit Schoonhoven, and Ronald JMM Does. Robust point location estimators for the ewma control chart. Quality Technology & Quantitative Management, 13(1):29–38, 2016.
[15] Rashid Mehmood, Kassimu Mpungu, Iftikhar Ali, Babar Zaman, Fawwad Hussain Qureshi, and Naveed Khan. A new approach for designing the shewhart-type control charts with generalized sensitizing rules. Computers & Industrial

This work is licensed under a Creative Commons Attribution-NonCommercial-NoDerivatives 4.0 License. For more information, see https://creativecommons.org/licenses/by-nc-nd/4

This article has been accepted for publication in IEEE Access. This is the author's version which has not been fully edited and
content may change prior to final publication. Citation information: DOI 10.1109/ACCESS.2024.3494042

Engineering, 182:109379, 2023.
[16] Douglas C Montgomery. The 100th anniversary of the control chart, 2024.
[17] John Lawson. An Introduction to Acceptance Sampling and SPC with R. CRC Press, 2021.
[18] Abdul Haq and Michael BC Khoo. An adaptive multivariate ewma chart. Computers & Industrial Engineering, 127:549–557, 2019.
[19] Aya A Aly, Nesma A Saleh, and Mahmoud A Mahmoud. An adaptive exponentially weighted moving average control chart for poisson processes. Quality Engineering, 33(4):627–640, 2021.
[20] Ross S Sparks. Cusum charts for signalling varying location shifts. Journal of Quality Technology, 32(2):157–171, 2000.
[21] Muhammad Noor-ul Amin, Afshan Riaz, and Amer Ibrahim Al-Omari. Adaptive exponentially weighted moving average control chart for monitoring process mean under ranked set sampling schemes. Iranian Journal of Science and Technology, Transactions A: Science, 45(5):1777–1787, 2021.
[22] Fan Yi and Peihua Qiu. An adaptive cusum chart for drift detection. Quality and Reliability Engineering International, 38(2):887–894, 2022.
[23] Abdul Haq and Faiqa Razzaq. New weighted adaptive cusum dispersion charts. Quality and Reliability Engineering International, 38(1):110–133, 2022.
[24] Aamir Saghir, Gadde Srinivasa Rao, Muhammad Aslam, and Azhar Ali Janjua. Pareto distribution-based shewhart control chart for early detection of process mean shifts. Journal of Statistical Theory and Applications, pages 1–18, 2024.
[25] Connie M Borror, Douglas C Montgomery, and George C Runger. Robustness of the ewma control chart to non-normality. Journal of quality technology, 31(3):309–316, 1999.
[26] Jyh-Jen Horng Shiau and Hsu Ya-Chen. Robustness of the ewma control chart to non-normality for autocorrelated processes. Quality Technology & Quantitative Management, 2(2):125–146, 2005.
[27] Hafiz Zafar Nazir, Muhammad Riaz, Ronald JMM Does, and Nasir Abbas. Robust cusum control charting. Quality Engineering, 25(3):211–224, 2013.
[28] Hafiz Zafar Nazir, Muhammad Riaz, and Ronald JMM Does. Robust cusum control charting for process dispersion. Quality and Reliability Engineering International, 31(3):369–379, 2015.
[29] Yu-Chang Lin, Chao-Yu Chou, and Chung-Ho Chen. Robustness of the ewma median control chart to non-normality. International Journal of Industrial and Systems Engineering, 25(1):35–58, 2017.
[30] Muhammad Abid, Hafiz Zafar Nazir, Muhammad Riaz, and Zhengyan Lin. In-control robustness comparison of different control charts. Transactions of the Institute of Measurement and Control, 40(13):3860–3871, 2018.
[31] Harold Manuel Madrid-Alvarez, Juan Carlos García-Díaz, and Víctor G Tercero-Gómez. A cusum control chart for gamma distribution with guaranteed performance. Quality and Reliability Engineering International, 40(3):1279–1301, 2024.
[32] Aamir Sanaullah, Aamir Majeed Chaudhary, Muhammad Hanif, and Prayas Sharma. Ewma control charts based on robust estimators: A powerful tool for monitoring a process with a non-normal distribution. Journal of Computational and Applied Mathematics, 449:115919, 2024.
[33] Muhammad Naveed, Muhammad Azam, Nasrullah Khan, Muhammad Aslam, Muhammad Saleem, and Muhammad Saeed. Control charts using half-normal and half-exponential power distributions using repetitive sampling. Scientific Reports, 14(1):226, 2024.
[34] Qurat-UL-Ain Khaliq and Muhammad Riaz. Robust tukey–cusum control chart for process monitoring. Quality and Reliability Engineering International, 32(3):933–948, 2016.
[35] Azaz Ahmed, Aamir Sanaullah, and Muhammad Hanif. A robust alternate to the hewma control chart under non-normality. Quality Technology & Quantitative Management, 17(4):423–447, 2020.
[36] Hafiz Zafar Nazir, Muhammad Abid, Noureen Akhtar, Muhammad Riaz, and Sadia Qamar. An efficient mixed-memory-type control chart for normal and non-normal processes. Scientia Iranica, 28(3):1736–1749, 2021.
[37] FF Gan. Design of optimal exponential cusum control charts. Journal of Quality Technology, 26(2):109–124, 1994.
[38] Mohammed S Shafae, Rebecca M Dickinson, William H Woodall, and Jaime A Camelio. Cumulative sum control charts for monitoring weibull-distributed time between events. Quality and Reliability Engineering International, 31(5):839–849, 2015.
[39] Harold Manuel Madrid-Alvarez, Juan Carlos García-Díaz, and Víctor G Tercero-Gómez. A cusum control chart for gamma distribution with guaranteed performance. Quality and Reliability Engineering International, 2023.
[40] AJJJ Bekker and JJJ Roux. Reliability characteristics of the maxwell distribution: A bayes estimation study. Communications in Statistics-Theory and Methods, 34(11):2169–2178, 2005.
[41] Hare Krishna, Vivekanand, and Kapil Kumar. Estimation in maxwell distribution with randomly censored data. Journal of Statistical Computation and Simulation, 85(17):3560–3578, 2015.
[42] Dan Li and Shuwei Miao. Fitting the wind speed probability distribution with maxwell and power maxwell distributions: A case study of north dakota sites. Sustainable Energy Technologies and Assessments, 47:101446, 2021.
[43] Vikas Kumar Sharma, Hassan S Bakouch, and Khushboo Suthar. An extended maxwell distribution: Properties and applications. Communications in Statistics-Simulation and Computation, 46(9):6982–7007, 2017.
[44] Hare Krishna and Manish Malik. Reliability estimation in maxwell distribution with type-ii censored data. International Journal of Quality & reliability management, 26(2):184–195, 2009.
[45] JS Rowlinson*. The maxwell–boltzmann distribution. Molecular Physics, 103(21-23):2821–2828, 2005.
[46] Hugo Hernandez. Standard maxwell-boltzmann distribution: definition and properties. ForsChem Research Reports, 2:2017–2, 2017.
[47] M Pear Hossain, M Hafidz Omar, and Muhammad Riaz. New v control chart for the maxwell distribution. Journal of Statistical Computation and Simulation, 87(3):594–606, 2017.
[48] M Pear Hossain, Ridwan A Sanusi, M Hafidz Omar, and Muhammad Riaz. On designing maxwell cusum control chart: an efficient way to monitor failure rates in boring processes. The International Journal of Advanced Manufacturing Technology, 100:1923–1930, 2019.
[49] M Pear Hossain and Muhammad Riaz. On designing a new vewma control chart for efficient process monitoring. Computers & Industrial Engineering, 162:107751, 2021.
[50] Faisal Shah, Zahid Khan, Muhammad Aslam, and Seifedine Kadry. Statistical development of the v_sq-control chart for extreme data with an application to the carbon fiber industry. Mathematical Problems in Engineering, 2021:1–11, 2021.
[51] Robert V Hogg, Joseph W McKean, and Allen T Craig. Introduction to mathematical statistics. Pearson, 2019.
[52] Tasuns: Manufacturing company of carbon fiber and carbon fiber composite products. 2024.
[53] Aliyu Ismail Ishaq and Alfred Adewole Abiodun. The maxwell–weibull distribution in modeling lifetime datasets. Annals of Data Science, 7(4):639–662, 2020.
[54] Talha Arslan, Sukru Acitas, and Birdal Senoglu. Parameter estimation for the two-parameter maxwell distribution under complete and censored samples. REVSTAT-Statistical Journal, 19(2):237–253, 2021.
[55] Salman Babayi and Esmaile Khorram. Inference of stress-strength for the type-ii generalized logistic distribution under progressively type-ii censored samples. Communications in Statistics-Simulation and Computation, 47(7):1975–1995, 2018.

This work is licensed under a Creative Commons Attribution-NonCommercial-NoDerivatives 4.0 License. For more information, see https://creativecommons.org/licenses/by-nc-nd/4

This article has been accepted for publication in IEEE Access. This is the author's version which has not been fully edited and
content may change prior to final publication. Citation information: DOI 10.1109/ACCESS.2024.3494042

[56] MG Bader and AM Priest. Statistical aspects of fibre and bundle strength in hybrid composites. Progress in science and engineering of composites, pages 1129–1136, 1982.
[57] Shubham Saini, Ajit Chaturvedi, and Renu Garg. Estimation of stress–strength reliability for generalized maxwell failure distribution under progressive first failure censoring. Journal of Statistical Computation and Simulation, 91(7):1366–1393, 2021.



ZAHID KHAN is currently working as a coresearch fellow in the Department of Quantitative Methods at the University of Pannonia, Hungary. He holds a permanent position as an Assistant Professor in the Department of Mathematics and Statistics at Hazara University, Pakistan. He earned his PhD from the University Technology PETRONAS, Malaysia, in 2017. His research interests encompass robust estimation in fuzzy probability distributions, neutrosophic statistics, and statistical methods for industrial process control. Dr. Zahid received a Talent Award Scholarship from the Higher Education Commission of Pakistan in 2006, a fellowship from Quaid-i-Azam University in 2007, and another fellowship from University Technology PETRONAS in 2013.



FAISAL SHAH holds the position of Senior Lecturer in Statistics at the Department of Mathematics, University of Haripur, KPK, Pakistan. He earned his M.Phil. degree in statistics from Riphah International University, Islamabad, Pakistan, in 2015. Currently, he is pursuing a Ph.D. in Statistics at Riphah International University, Islamabad. His research focuses on statistical process control and reliability analysis.

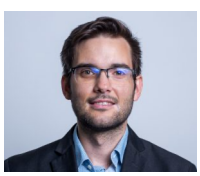

ATTILA I. KATONA is a senior research fellow at the Department of Quantitative Methods, Faculty of Business and Economics, University of Pannonia and a former data scientist at IBM. His research interests include the treatment of decision risks arising from measurement uncertainty in quality control and statistical control chart design. His experiences are associated with Management Science and Operations Research and big data approaches. Attila has valuable publications in the journals Expert Systems with Applications and Computers & Industrial Engineering, and he is a recipient of the Pro Scientia Golden Medal from the Hungarian Academy of Sciences.



ZSOLT T. KOSZTYAN is a full professor and head of the Department of Quantitative Methods at the University of Pannonia. His research interest is the development of methodologies to handle complex management problems and systems related to mathematical models and algorithms for project management, production, maintenance, and network science. This research area is at the top of three intersecting fields: management science, applied informatics, and applied network science. He worked as a senior research fellow at the Institute of Advanced Studies, KRAFT Social Innovation Lab, and at the MTA-PE (Hungarian Academy of Sciences-University of Pannonia) Budapest Ranking Research Group. He is a single or corresponding author of more than 200 publications, including three books.

This work is licensed under a Creative Commons Attribution-NonCommercial-NoDerivatives 4.0 License. For more information, see https://creativecommons.org/licenses/by-nc-nd/4